2022 44th Annual International Conference of
the IEEE Engineering in Medicine & Biology Society (EMBC)
Scottish Event Campus, Glasgow, UK, July 11-15, 2022

2022 44th Annual International Conference of the IEEE Engineering in Medicine & Biology Society (EMBC) | 978-1-7281-2782-8/22/$31.00 ©2022 IEEE | DOI: 10.1109/EMBC48229.2022.9871850

Concept and first Implementation of an intracochlearly navigated Electrode Array for Cochlear Implantation

Christian W. D. Scheunemann, Johannes Taeger, Sandra V. Brecht, Tilmann Neun, Rudolf Hagen, Tim C. Lueth and Kristen J. Rak

Abstract— **Cochlear implants (CI) are an established treatment for people with deafness or severe hearing loss. To restore patients' hearing an electrode array (EA) of the CI is inserted into the cochlea to stimulate the auditory nerve. Thereby, the exact positioning and gentle insertion of the EA is crucial for optimal hearing perception outcome. Currently, only microscopic vision is available for entering the cochlea, but the critical intracochlear process during EA insertion is like a "black box" and the surgeon has to rely on haptic feedback. Methods for visualizing the insertion process during surgery are inaccurate or not suitable for routine use due to radiation exposure. To address this problem, we developed a computer-assisted and image-guided cochlear implantation system with an exact real-time visualization of the EA position during the insertion process. The system is based on an electromagnetic tracking system that measures the position and orientation of a sensor integrated into the tip of a EA prototype and visualizes it in presurgical image data. A first experiment with our system showed that a EA prototype could be inserted into a cochlea of a human temporal bone and placed with an accuracy of 1.1 mm ± 0.4 mm. A maximum insertion angle of 120° was achieved.**

I. Introduction

A cochlear implant (CI) is an implantable prosthesis used to restore hearing in cases of profound hearing loss or deafness. In 2019, over 736.000 patients worldwide have received a CI, 183.000 of them alone in the United States [1]. The cochlear implant has an electrode array (EA) which is inserted into the cochlea, preferentially in the scala tympani (ST), where it directly stimulates the auditory nerve fibers bypassing the inner ear structures. For optimal hearing perception outcome in cochlear implantation, it is not only essential to select the correct EA to obtain appropriate cochlear coverage [2-5], but also to prevent damage to intracochlear structures [5-8]. A preoperative selection of an anatomically most suitable EA appears to be important to achieve the best possible postoperative speech understanding. In addition to tone audiometric and anamnestic prediction methods [9, 10], it is currently assumed that tonotopic stimulation of the cochlea leads to an improvement in speech understanding [11, 12]. The EA is inserted manually by the surgeon under microscopic vision. Some EA are equipped with special insertion tools like tubes or stylets that stabilize and guide the EA. During insertion, the surgeon cannot see the EA inside the cochlea and has to rely on haptic feedback. Since the actual insertion depth of the EA can differ from the predefined depth, the correct placement of the EA must be verified by radiography or X-ray tomography so, if necessary, the EA can be repositioned [13].

A. State of the art and research

For improving the EA placement and cochlea implantation, many different methods have been developed. To enhance the electrical stimulation of the nerve fibers, preformed EA have been developed to achieve a positioning of the EA closer to the modiolus [14, 15]. With post-surgical and intra-surgical impedance measurements of electrically evoked compound action potentials (eCAP) [16-19] or electrocochleography (eCochG) [20] via the EA, changes in the position of the EA were recognized and indications of residual hearing were determined [21]. Pre-surgical insertion depth calculation allowed the surgeon to find the correct insertion depth to take advantage of the tonotopy of the cochlea [22]. Through intra-surgical stenvers imaging [23] or fluoroscopy [24] a real time visualization of the EA insertion process was realized. Another approach to reduce trauma and optimize positioning of the cochlear implant is to make the electrode controllable [25]. In one approach, small magnets were integrated into the tip of the EA so that it could be manipulated via an external magnetic field, resulting in a reduction in force on the walls of the cochlea [26]. By inserting a Kevlar wire into the EA, it was possible to bend it specifically and follow the coil better during insertion and thus be inserted more gently [27]. By integrating fluid-filled chambers into the EA, the bending of the EA during insertion was adapted to the cochlear bending by varying the pressures in the chambers [28]. In addition, instruments have been developed that actively control the insertion of the EA from outside, so-called insertion tools. These grip the EA outside the cochlea and carry out the insertion process in a controlled and partially automated manner. Manual [29], mechanical [30] and hydraulic [31] systems have been developed for this purpose. A first approach for navigating an EA was realized by Klafas et al. (2014) as a 10:1 scaled model of an EA array with several embedded coils. The shapes of this model could be measured with the help of three orthogonal Helmholtz coils surrounding the model inducing currents in the embedded coils. The contour was then visualized in MATLAB plots [32]. Kukushev (2018) also mentioned a concept for a navigated EA in which the position is determined by an electromagnetic tracking system and visualized in medical images [33].

Christian W. D. Scheunemann, Sandra V. Brecht and Tim C. Lueth are with the Institute of Micro Technology and Medical Device Technology, Technical University of Munich, Garching, Germany.
(email: christian.scheunemann@tum.de)

Johannes Taeger, Rudolf Hagen and Kristen J. Rak are with the Comprehensive Hearing Center, Department of Oto-Rhino-Laryngology, University of Wuerzburg, Wuerzburg, Germany.

Tilmann Neun is with the Institute for Diagnostic and Interventional Neuroradiology, University of Wuerzburg, Wuerzburg, Germany.

B. Limitation of the state of the art and research

Despite all the developments to improve the quality of cochlea implant fitting, there is still the major problem that the intracochlear process is like a "black box" during the insertion of the EA. This is due to the fact that a direct optical visualization of the EA in the cochlea is not possible. Pre-surgical calculation and preformed EA help the surgeon to estimate the insertion depth or place the EA closer to the modiolus. However, they do not allow a real-time visualization or control of the insertion process. Real-time visualization of the insertion process can currently only be achieved indirectly through electrophysiological measurements like eCAP or eCochG, but these do not indicate the position of the EA, only the interaction of the electrodes with the tissue [18] or the functionality of the cochlea [34]. Direct real time visualization of the position is possible with radiological techniques, but these increase the radiation exposure of patients and surgeons. The state of research shows some promising and highly innovative projects for navigating and manipulating the EA during insertion, which have also been realized as prototypes. The aforementioned methods for navigating the EA show possibilities, to visualize the EA during the insertion, but they are still at an early stage. Approaches to control the insertion of the EA, such as systems that can manipulate the EA tip via a magnet, have fillable cavities, pre-bent and manipulable wires, or automatic insertion tools allow easier insertions. However, all these systems lead to an increased stiffness of the EA due to the altered mechanical properties of the EA [25]. They also do not solve the main problem in cochlear implantation, which is the lack of real-time visualization during insertion. Furthermore, these systems could be improved if they were supplemented by a sensor system for orientation as well as for targeted control of the EA [25]. Thus, an exact real-time visualization of the position of the EA during the insertion process, which would also allow immediate placement control and repositioning, is not yet sufficiently possible.

C. Research Goal

Our goal is to develop a computer-assisted and image-guided cochlear implantation system with an exact real-time visualization of the electrode array position in pre-surgical image data during the insertion process which allows the surgeon an immediate placement control and the possibility of intra-surgical repositioning. The presented study is a first step in the development process to prove the applicability of the intracochlear navigation of an experimental EA for the first time.

II. Materials and Methods

A. Concept

The concept of the system is shown in Fig. 1. It consists of a processing unit with a navigation software (1) which is connected to an electromagnetic (EM) tracking unit (2). This EM tracking unit generates a defined alternating electromagnetic field in the surgical area (7) via a field generator (9). This EM field induces currents in a sensor integrated into a reference (10) and in a sensor integrated into the tip (11) of an electrode array (4) of the cochlea implant (3). By connecting the reference and the cochlea implant to the EM tracking unit, these currents can be measured, and the position and orientation of the sensors calculated. The reference serves as a reference point for the registration of the patient and has therefore to be firmly attached to the head. This and with measuring the pose of the EA tip relative to the reference also ensures that intentional or unintentional movement of the head does not affect the accuracy of the measurement. After registration of the patient, the position and orientation of the EA's tip relative to the patient can be visualized in pre-surgical CT and/or MRI image data (12) in real time. This allows the surgeon to control the insertion depth and angle of the EA into the cochlea (5). Moreover, misinsertion or misplacement is directly visible and there is the possibility to correct the placement of the EA during surgery.

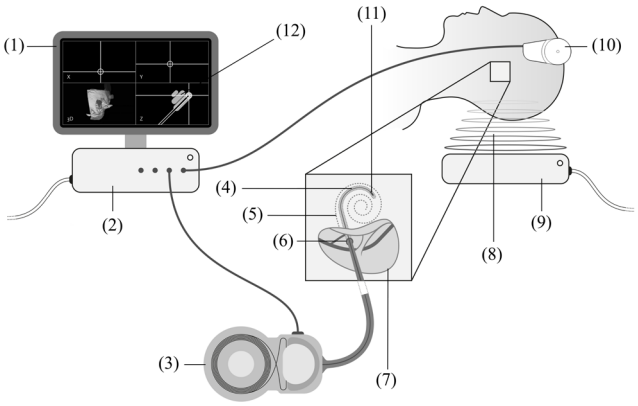

Fig. 1. Concept of the navigated cochlea implantation: (1) processing unit with the navigation software, (2) EM tracking unit, (3) cochlear implant, (4) electrode array, (5) cochlea, (6) cochleostomy/round window (7) surgical area, (8) electromagnetic field, (9) field generator, (10) patient reference, (11) sensor integrated into the tip, (12) user interface with visualization of the insertion.

B. Requirements

Mean insertion angles for soft surgery implantations are between 270 degrees to 420 degrees and for deep insertion techniques, angles are from 405 degrees to 630 degrees [35]. Considering the anatomy of the cochlea, the dimensions of the scales and the known characteristics of the CI electrodes currently available on the market, the dimensions of the sensor (diameter and length) are determined as follows:

Diameter: The scala tympani has an average height H_{ST} of 0.86 mm in the area of the second turn [36]. In order not to increase the risk of trauma during insertion, the diameter d of the sensor should not exceed half of the height and should therefore be in the range of 0.4 mm maximum. This means that it would have approximately the diameter of 0.3 - 0.5 mm at the tip as currently used EA which allows atraumatic insertion. In addition, these diameters could also be inserted into the topmost turn, which has an average height H_{ST} of 0.61 mm [36].

Length: To estimate the insertable sensor length, into the scala tympani, the sensor can be considered as a rigid cylinder with diameter d and length l. This cylinder is inserted into a tube with the width of the scala tympani B_{ST} (B_{ST} second turn 1.46 mm) and the height of the scala tympani H_{ST} (H_{ST} second turn 0.86 mm). Since the pitch of the cochlea is very small compared to the radius of its turn, the arc of the turn can be seen as the limiting factor. The outer radius R_A of the arc of the turn corresponds to half the width of the cochlea B_C (B_C second turn 3.8 mm [37]) and the inner radius R_I results from R_A - B_{ST}.

If d of the cylindric sensor is smaller than H_{ST} and B_{ST}, when looking at the cross-section of the scala tympani tube from above (similar to Stenvers/Cochlea View), the maximum length of the cylinder can be calculated using the Pythagorean theorem (1).

$$l = 2\sqrt{R_A^2 - (d + (R_A - B_{ST}))^2} \quad (1)$$

From (1) and the dimensions of the cochlea, it follows that e.g., a sensor with 0.3 mm diameter, which should be inserted in the middle/second turn of the cochlea, should not exceed a maximum length of 3.50 mm. If the diameter is 0.4 mm, the maximum length should only be 3.41 mm.

C. Implementation

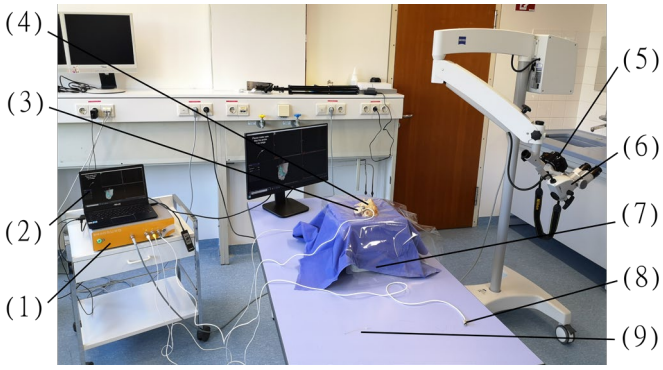

Fig. 2. Experimental setup: (1) EM tracking unit, (2) Processing Unit, (3) reference, (4) specimen, (5) camera, (6) microscope, (7) field generator, (8) EA adapter cable, (9) electrode array prototype (close-up in Fig. 3.)

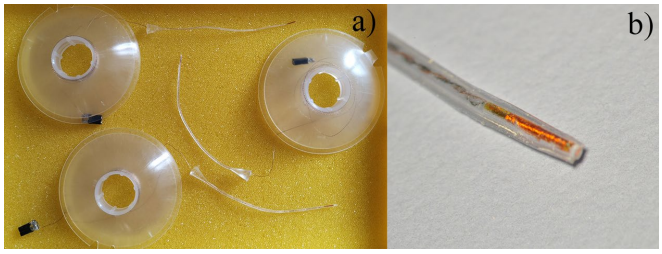

Fig. 3. a) electrode array prototypes with cable and connector, b) close-up of the electrode array tip with integrated sensor

Fig. 2. shows the implementation of the system for the experimental setup. The processing unit (2) was an Asus UX331U notebook (ASUStek Computer Inc., Taipeh, Taiwan) with a modified navigation software for ENT-surgery (Ergosurg GmbH, Ismaning, Germany). The EM tracking unit (1) is based on the Aurora EM-System from NDI (Northern Digital, Waterloo, Canada) with an NDI Planar Field Generator 20-20 (7). As reference an Ergosurg Patient tracker (3) with an integrated 6DoF sensor was used. The mentioned navigation software processes the measurements of the NDI tracking system and allows pre-surgical planning of waypoints, landmarks and risk-structures in imported medical image data. It provides landmark or surface registration of the patient and real time visualization of sensors and instruments in medical images. For the system presented, the software was modified to support the sensor used in the EA prototype, visualize the sensor's dimensional shape, and provide real-time measurement of the distance between the sensor and landmarks/measurement points. An adapter cable with a 2-pole connector (8) was constructed as the connection between the EA prototype (9) and the EM tracking system. In Fig. 3. a) the EA prototype and in Fig. 3. b) a close-up view of the prototype's tip with the integrated sensor are shown. As sensor for the prototype, the smallest commercially available 5 DoF sensor for EM tracking (part no.: 610159, NDI, Waterloo, Canada) with a diameter of 0.41 mm and a length of 4.9 mm was used. The sensor was encapsulated in a biocompatible silicone shell with a hardness of 75 shore A (part no.: MED-6019, Nusil, Avantor, Philadelphia, USA) in the shape of an EA. The shape, dimension and flexibility of the prototype were designed to be similar to commercially available EA with regard to the integration of the sensor. Its diameter tapers from 1 mm at the base to 0.5 mm at the tip. With a length of 70 mm, it is slightly longer than a normal EA, to allow later fixation in the experiments. The mold for the prototype was designed in Catia V5 (Dassault Systèmes, Vélizy-Villacoublay, France) and manufactured with a Form 2 Stereolithography (SLA) 3D printer (Formlabs, Somerville, Massachusetts, USA). As the material for the mold, the Formlabs clear resin with a print resolution of 25 microns was used.

III. Experiment

In the presented experiment (setup in Fig. 2.), the implemented system and an EA prototype was tested for navigability, insertability and accuracy of positioning the EA in the cochlea of a human temporal bone. In addition to the aforementioned system, a calibrated registration probe (Ergosurg GmbH, Ismaning, Germany) was used for registration of the specimen, and an OPMI Pico microscope (Carl Zeiss AG, Jena, Germany) (6) and a Nikon D90 camera (Nikon AG, Tokyo, Japan) (5) were used for documentation.

1) Specimen: For this study, a fresh frozen human temporal bone specimen (4) was used. The study was conducted in concordance with local guidelines and principles of the Declaration of Helsinki and Good Clinical Practice.

2) Preparation: The temporal bone was thawed at room temperature and then immersed in saline solution (0.9 %) for about 3 h. A posterior tympanotomy was drilled after a cortical mastoidectomy. The round window was exposed by removing the crista fenestrae. Four self-drilling titanium screws were inserted as fiducial markers superior, anterior, posterior and inferior of the mastoidectomy. In addition, three X-ray markers were placed at the sigmoid sinus, the bone of the dura of the middle fossa and the lateral semicircular canal. For probing, the screw heads had a touchable inner diameter of 1.0 mm and the X-ray markers of 1.15 mm.

3) Imaging: A flat panel detector volumetric computed tomography (fpVCT) was performed on a C-arm (Axiom Artis) with a commercially available software Syngo (Siemens Healthineers AG, Erlangen, Germany). The datasets were acquired using the following parameters: 20s DCT Head protocol; tube voltage = 109 kV; tube current = 21 mA; pulse length = 3.5 ms; rotation angle = 200°; frame angulation step = 0.5°/frame. Post-processing was performed with the following settings: 512 x 512 section matrix; HU kernel types; sharp image characteristics; slice thickness = 99 µm. The fpVCT images were rotated in the cochlear view in HOROS software and exported as DICOM.

4) Planning: The DICOM images were loaded into the navigation software and its planning tool was used to manually place registration points in all spatial planes on the screw heads

(fiducial markers) as well as measurement points on the X-ray markers and the round window.

5) Registration: The four fiducial markers were touched by the calibrated registration probe for registration of the specimen. After a successful registration, the fiducial registration error (FRE) / RMS x_{FRE} was measured.

6) Test of navigation accuracy: The fiducial markers and the X-ray markers were touched with the registration probe to measure the accuracy of the registration. The fiducial markers, the X-ray markers and the round window were touched with the tip of the EA to measure the accuracy of the EA prototype. By measuring the Euclidean distance between the center of the registration/measurement points and the tip of the EA, the navigation error / target registration error (TRE) x_{TRE} could be calculated according to equation (2).

$$x_{TRE} = {}^{model}T_{patient}\,{}^{patient}T_{sensor}\,{}^{sensor}p_{EA\,Tip} - {}^{model}p_{measuring\,point} \quad (2)$$

7) Insertion of the EA prototype: Steps 5) and 6) were repeated nine times before the EA prototype was manually inserted in the scala tympani after opening the round window membrane. The insertion process was stopped, after no further insertion of the EA was possible. Afterwards, the EA was fixed in the round window niche with glue and screenshots of the navigation with the visualized EA position were taken.

8) Postoperative analysis: After the navigation, another fpVCT of the temporal bone specimen with affixed EA prototype was made. This fpVCT was also processed for comparability according to step 3). The two fpVCT, the one from the navigation and the one with affixed EA were fused in the navigation software and the measured position of the EA tip was marked with a crosshair. A visualized circle with a radius of 1 mm in the center of the crosshair represents an error of 1 mm around the calculated position. If the actual EA tip is within this circle, an accuracy of 1 mm could be assumed.

IV. Results

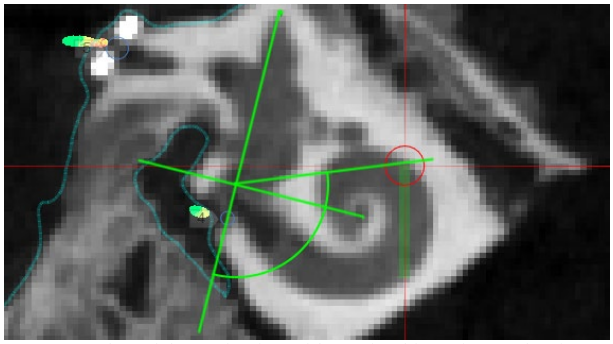

Fig. 4. Screenshot of the navigation with maximal insertion angle of 120°.

The experiment showed that the EA prototype could be inserted into a human cochlea and visualized in real-time in medical image data during insertion. The data of the nine measurements resulted in a mean FRE of the navigation $\bar{x}_{FRE}$ of 0.24 mm and a maximum measured error $x_{FRE,max}$ of 0.44 mm. The mean TRE of the EA prototype $\bar{x}_{TRE}$ was 1.1 mm with a standard deviation s_{TRE} of 0.4 mm. The maximum measured error $x_{TRE,max}$ was 2.0 mm. With the sensor used in the EA, a maximum insertion angle of approximately 120° was achieved (Fig. 4.). The comparison between the visualized and the actual position of the EA is shown in Fig. 5. The red circle in Fig. 5. b) has a radius of 1 mm and is placed at the calculated position of the tip in Fig. 5. a). The tip of the actual EA lies within the red circle and confirms the measured $\bar{x}_{TRE}$ of 1.1 mm.

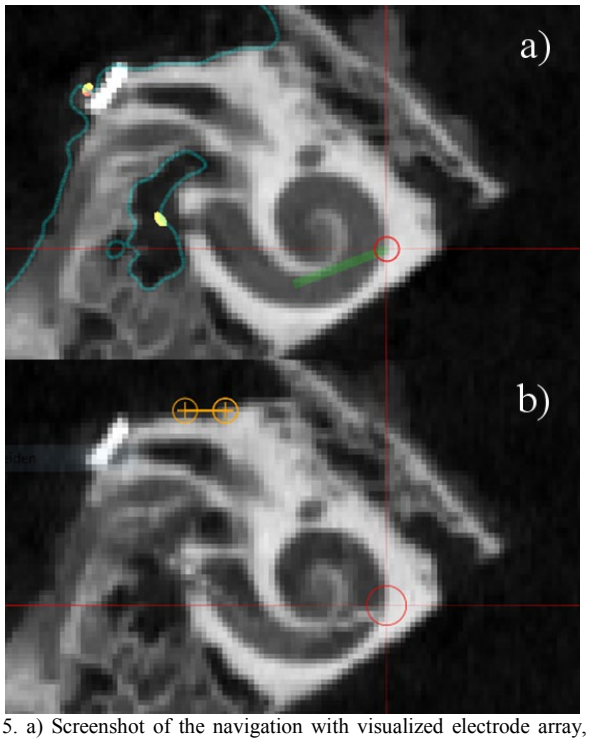

Fig. 5. a) Screenshot of the navigation with visualized electrode array, b) actual position of the electrode array in the same layer as a) (second fpVCT). The tip of the electrode array in b) lies within the 1 mm radius of the red circle which confirms the measured accuracy of 1.1 mm ± 0.4 mm.

V. Discussion & Conclusion

In this paper, we described a new concept and first implementation of an intracochlearly navigated electrode array for cochlear implantation. Our experiment demonstrates that an EA prototype with an integrated sensor can be inserted into the human cochlea and placed with an accuracy of 1.1 mm ± 0.4 mm. The system allows an exact real-time visualization of the EA's position during the insertion process. In this way, the surgeon has immediate placement control and the possibility of repositioning the EA. The measured positioning accuracy was confirmed by comparing the calculated and real positions of the prototype. The maximum insertion angle of the EA prototype was 120°. However, this insertion depth is not yet deep enough for normal or soft surgery cochlear implantation. As described above, the limiting factor is the dimension of the sensor in the tip of the EA. Therefore, the next step is to develop a sensor with smaller dimensions that can be inserted deeper into the cochlea. Furthermore, the accuracy achieved, may not be sufficient for an accurate EA placement. Thus, inaccuracies in manually setting the registration points / measurement points in the image data could be reduced through automatic registration methods, for example a maxilla splint with integrated x-ray markers for the patient. In addition, if the EM sensor is integrated directly into the EA, the interactions of the sensor with the functionality of the implant or with

postoperative diagnoses must be considered. It is unknown how the sensor coil will influence the spread of excitation through the implant and may cause disturbance in in vivo functionality or how the sensor will interact with magnetic resonance imaging systems where metal parts and coils could potentially get hot or be moved by magnetic forces. Here, further investigations need to be undertaken.

ACKNOWLEDGMENT

The authors thank Ergosurg GmbH for the technical support and providing the EM tracking equipment.

REFERENCES

[1] NIDCD, "Cochlear Implants," *National Institute on Deafness Other Communication Disorders Fact Sheet Hearing and Balance*, NIH Publication No. 00-4798, 2021.

[2] A. Buchner, A. Illg, O. Majdani, and T. Lenarz, "Investigation of the effect of cochlear implant electrode length on speech comprehension in quiet and noise compared with the results with users of electro-acoustic-stimulation, a retrospective analysis," *PLoS One*, vol. 12, no. 5, 2017.

[3] I. Hochmair, W. Arnold, P. Nopp, C. Jolly, J. Muller, and P. Roland, "Deep electrode insertion in cochlear implants: apical morphology, electrodes and speech perception results," *Acta Otolaryngol*, vol. 123, no. 5, pp. 612-7, Jun, 2003.

[4] B. P. O'Connell, A. Cakir, J. B. Hunter, D. O. Francis, J. H. Noble, R. F. Labadie, G. Zuniga, B. M. Dawant, A. Rivas, and G. B. Wanna, "Electrode Location and Angular Insertion Depth Are Predictors of Audiologic Outcomes in Cochlear Implantation," *Otol Neurotol*, vol. 37, no. 8, pp. 1016-23, Sep, 2016.

[5] B. P. O'Connell, J. B. Hunter, D. S. Haynes, J. T. Holder, M. M. Dedmon, J. H. Noble, B. M. Dawant, and G. B. Wanna, "Insertion depth impacts speech perception and hearing preservation for lateral wall electrodes," *Laryngoscope*, vol. 127, no. 10, pp. 2352-57, 2017.

[6] O. Adunka, and J. Kiefer, "Impact of electrode insertion depth on intracochlear trauma," *Otolaryngol Head Neck Surg*, vol. 135, no. 3, pp. 374-82, Sep, 2006.

[7] C. A. Buchman, M. T. Dillon, E. R. King, M. C. Adunka, O. F. Adunka, and H. C. Pillsbury, "Influence of cochlear implant insertion depth on performance: a prospective randomized trial," *Otol Neurotol*, vol. 35, no. 10, pp. 1773-9, Dec, 2014.

[8] M. C. Suhling, O. Majdani, R. Salcher, M. Leifholz, A. Buchner, A. Lesinski-Schiedat, and T. Lenarz, "The Impact of Electrode Array Length on Hearing Preservation in Cochlear Implantation," *Otol Neurotol*, vol. 37, no. 8, pp. 1006-15, Sep, 2016.

[9] S. Dazert, J. P. Thomas, A. Loth, T. Zahnert, and T. Stover, "Cochlear Implantation," *Dtsch Arztebl Int,* vol. 117, no. 41, pp. 690-700, 2020.

[10] U. Hoppe, T. Hocke, A. Hast, and H. Iro, "Cochlear Implantation in Candidates With Moderate to Severe Hearing Loss and Poor Speech Perception," *Laryngoscope*, vol. 131, no. 3, pp. E940-E945, 2021.

[11] I. Hochmair, E. Hochmair, P. Nopp, M. Waller, and C. Jolly, "Deep electrode insertion and sound coding in cochlear implants," *Hear Res*, vol. 322, pp. 14-23, Apr, 2015.

[12] A. J. Oxenham, J. G. Bernstein, and H. Penagos, "Correct tonotopic representation is necessary for complex pitch perception," *Proc Natl Acad Sci USA*, vol. 101, no. 5, pp. 1421-5, Feb 3, 2004.

[13] T. Lenarz, "Cochlear implant - state of the art," GMS Curr Top Otorhinolaryngol Head Neck Surg, vol. 16, 2017.

[14] J. T. Roland, Jr., "A model for cochlear implant electrode insertion and force evaluation: results with a new electrode design and insertion technique," *Laryngoscope*, vol. 115, no. 8, pp. 1325-39, Aug, 2005.

[15] F. Hassepass, S. Bulla, W. Maier, R. Laszig, S. Arndt, R. Beck, L. Traser, and A. Aschendorff, "The new mid-scala electrode array: a radiologic and histologic study in human temporal bones," *Otol Neurotol*, vol. 35, no. 8, pp. 1415-20, Sep, 2014.

[16] R. K. Shepherd, S. Hatsushika, and G. M. Clark, "Electrical stimulation of the auditory nerve: the effect of electrode position on neural excitation," *Hear Res*, vol. 66, no. 1, pp. 108-20, Mar, 1993.

[17] P. Mittmann, A. Ernst, and I. Todt, "Intraoperative Electrophysiologic Variations Caused by the Scalar Position of Cochlear Implant Electrodes," *Otol Neurotol*, vol. 36, no. 6, pp. 1010-4, Jul, 2015.

[18] F. A. Di Lella, D. De Marco, F. Fernandez, M. Parreno, and C. M. Boccio, "In Vivo Real-time Remote Cochlear Implant Capacitive Impedance Measurements: A Glimpse Into the Implanted Inner Ear," *Otol Neurotol*, vol. 40, no. 5S Suppl 1, pp. S18-S22, Jun, 2019.

[19] Z. Yaniv, E. Wilson, D. Lindisch, and K. Cleary, "Electromagnetic tracking in the clinical environment," *Med Phys*, vol. 36, no. 3, pp. 876-92, Mar, 2009.

[20] A. Dalbert, F. Pfiffner, C. Roosli, K. Thoele, J. H. Sim, R. Gerig, and A. M. Huber, "Extra- and Intracochlear Electrocochleography in Cochlear Implant Recipients," *Audiol Neuro-otol*, vol. 20, no. 5, pp. 339-48, 2015.

[21] S. Haumann, M. Imsiecke, G. Bauernfeind, A. Buchner, V. Helmstaedter, T. Lenarz, and R. B. Salcher, "Monitoring of the Inner Ear Function During and After Cochlear Implant Insertion Using Electrocochleography," *Trends Hear*, vol. 23, Jan-Dec, 2019.

[22] D. Schurzig, M. E. Timm, C. Batsoulis, R. Salcher, D. Sieber, C. Jolly, T. Lenarz, and M. Zoka-Assadi, "A Novel Method for Clinical Cochlear Duct Length Estimation toward Patient-Specific Cochlear Implant Selection," *OTO open*, vol. 2, no. 4, 2018.

[23] B. Carelsen, W. Grolman, R. Tange, G. J. Streekstra, P. van Kemenade, R. J. Jansen, N. J. Freling, M. White, B. Maat, and W. J. Fokkens, "Cochlear implant electrode array insertion monitoring with intra-operative 3D rotational X-ray," *Clin Otolaryngo*l, vol. 32, no. 1, pp. 46-50, Feb, 2007.

[24] A. Aschendorff, "Imaging in cochlear implant patients," GMS current topics in otorhinolaryngology, head and neck surgery, vol. 10, 2011.

[25] T. S. Rau, S. Hügl, T. Lenarz, and O. Majdani, "Toward steerable electrodes. An overview of concepts and current research," *Current Directions in Biomedical Engineering*, vol. 3, no. 2, pp. 765-9, 2017.

[26] R. J. Clark, L. Lisandro, W. M. Frank, and J. J. Abbott, "Investigation of magnetic guidance of cochlear implants," *IROS'11- IEEE/RSJ International Conference on Intelligent Robots and Systems*, 2011.

[27] J. Zhang, and N. Simaan, "Design of Underactuated Steerable Electrode Arrays for Optimal Insertions," *Journal of Mechanisms and Robotics*, vol. 5, no. 1, 2013.

[28] B. Arcand, S. Shyamsunder, and C. Friedrich, "A Fluid Actuator for Thin-Film Electrodes," *Journal of Medical Devices*, pp. 70-78, 2007.

[29] L. B. Kratchman, D. Schurzig, T. R. McRackan, R. Balachandran, J. H. Noble, R. J. Webster, 3rd, and R. F. Labadie, "A manually operated, advance off-stylet insertion tool for minimally invasive cochlear implantation surgery," *IEEE Trans Biomed Eng*, vol. 59, no. 10, pp. 2792-800, Oct, 2012.

[30] A. Hussong, T. Rau, H. Eilers, S. Baron, B. Heimann, M. Leinung, T. Lenarz, and O. Majdani, "Conception and design of an automated insertion tool for cochlear implants," *Annu Int Conf IEEE Eng Med Biol Soc*, vol. 2008, pp. 5593-6, 2008.

[31] T. S. Rau, M. G. Zuniga, R. Salcher, and T. Lenarz, "A simple tool to automate the insertion process in cochlear implant surgery," *Int J Comput Assist Radiol Surg*, Aug 28, 2020.

[32] C. Klafas, A. McEwan, and P. Carter, "Design of an intra-operative imaging system for the cochlear implant," *Annu Int Conf IEEE Eng Med Biol Soc*, pp. 2448-51, 2014.

[33] G. Kukushev, "Navigierte Cochlea-Implantat-Elektrode," Forschung heute – Zukunft morgen, *Thieme Laryngo-Rhino-Otologie*, 2018.

[34] A. Radeloff, W. Shehata-Dieler, A. Scherzed, K. Rak, W. Harnisch, R. Hagen, and R. Mlynski, "Intraoperative monitoring using cochlear microphonics in cochlear implant patients with residual hearing," *Otol Neurotol*, vol. 33, no. 3, pp. 348-54, Apr, 2012.

[35] A. Aschendorff, J. Kromeier, T. Klenzner, and R. Laszig, "Quality control after insertion of the nucleus contour and contour advance electrode in adults," *Ear and hearing*, vol. 28, no. 2, pp. 75–79, 2007.

[36] K. Braun, F. Böhnke, and T. Stark, "Three-dimensional representation of the human cochlea using micro-computed tomography data: Presenting an anatomical model for further numerical calculations," *Acta Oto-Laryngologica,* vol. 132, no. 6, pp. 603-613, 2012.

[37] E. Erixon, H. Högstorp, K. Wadin, and H. Rask-Andersen, "Variational Anatomy of the Human Cochlea: Implications for Cochlear Implantation," *Otology & Neurotology*, vol. 30, no. 1, pp. 14-22, 2009.